

# Study on Smectic Liquid Crystal Glass and Isotropic Liquid Glass Formed by Thermotropic Main-Chain Liquid Crystal Polyester

Masatoshi Tokita,\* Shin-ichiro Funaoka, and Junji Watanabe

Department of Organic and Polymeric Materials, Tokyo Institute of Technology, Ookayama, Meguro-ku, Tokyo 152-8552, Japan

Received June 21, 2004; Revised Manuscript Received October 21, 2004

**ABSTRACT:** Two distinct glassy states formed by a thermotropic main-chain BB-3(1-Me) polyester were characterized by the wide-angle X-ray diffraction and DSC methods. In the BB-3(1-Me), a smectic CA liquid crystal (LC) was formed from an isotropic liquid on gradual cooling at rates smaller than  $1\text{ }^{\circ}\text{C min}^{-1}$  and solidified without crystallization, resulting in the smectic LC glass. On the other hand, the isotropic liquid solidified without the liquid crystallization on rapid cooling at rates larger than  $50\text{ }^{\circ}\text{C min}^{-1}$ , resulting in the isotropic liquid glass. On heating, the smectic LC glass showed a glass transition ( $T_g^{\text{LC}}$ ) of  $81\text{ }^{\circ}\text{C}$ , while the isotropic liquid glass showed a glass transition ( $T_g^{\text{iso}}$ ) of  $93\text{ }^{\circ}\text{C}$  and transformed to the smectic LC at  $110\text{ }^{\circ}\text{C}$ . The corresponding heat capacity increases were  $50.1$  and  $78.5\text{ J mol}^{-1}\text{ K}^{-1}$  for the smectic LC glass and the isotropic liquid glass, respectively. The enthalpy–temperature relationship in all the states was estimated by integration of the heat capacity measured by the temperature-modulated DSC method. Temperature dependences of the enthalpy relaxation time of the two glasses obey the Vogel–Fulcher–Tamman (VFT) relationship and clearly show a single ideal glass temperature  $T_0^{\text{LC}} (= 342\text{ K})$  for the smectic LC, but two ideal glass temperatures  $T_{0\text{L}}^{\text{iso}} (= 343\text{ K})$  and  $T_{0\text{H}}^{\text{iso}} (= 353\text{ K})$  for the isotropic liquid.  $T_{0\text{L}}^{\text{iso}}$  is  $10\text{ K}$  lower than  $T_{0\text{H}}^{\text{iso}}$  and corresponds to  $T_0^{\text{LC}}$ . According to a mode coupling theory of the glass transition of hard ellipsoid molecule liquid, the glass transition of the isotropic liquid at  $T_{0\text{L}}^{\text{iso}}$  is associated with the freezing of translation molecular motions, while the transition at  $T_{0\text{H}}^{\text{iso}}$  with the freezing of molecular orientation fluctuation. The correspondence of  $T_0^{\text{LC}}$  to  $T_{0\text{L}}^{\text{iso}}$  suggests that the glass transition of the smectic LC is dominated by the freezing of translation molecular motions in the smectic layer direction.

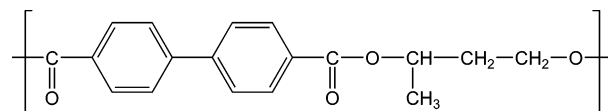
## Introduction

Thermotropic liquid crystal materials form isotropic liquid, liquid crystal, and crystal phases in an order of decreasing temperature. Some of them solidify without crystallization and form the solid which possesses the structure identical to the preceding liquid crystal. On heating, the solid shows a jump in the specific heat and a sudden decrease in the elastic constant at a temperature just like the conventional amorphous glassy materials. The solid state has been found for low molecular weight liquid crystal materials as well as polymeric ones and regarded as liquid crystal glass.<sup>1–16</sup> While the conventional glass, namely isotropic liquid glass, is characterized by an absence of long-range order, the liquid crystal glass possesses the long-range order identical to the preceding liquid crystal. The nematic liquid crystal glass is described by a simple orientational order of rodlike molecules. The smectic liquid crystal glass has layered structure, in other words, long-range one-dimensional positional order as well as the orientational order. These liquid crystal glasses are thus expected to provide new insight into dynamics of glassy materials representing a topic of current interest in condensed matter physics.

As a first attempt, it is interesting to compare the glass transition behavior between the LC and isotropic liquid glasses. However, a few attempts have been made to show difference in thermal and dynamic properties between these two glassy states. A main reason is that there have been few materials forming both the liquid crystal glass and the isotropic liquid glass.<sup>5,6,14,15</sup> The

liquid crystallization from the isotropic melt generally takes place close to equilibrium: it is less dependent on cooling rate in both the transition temperature and the enthalpy change. It is thus usual that the isotropic melt transforms to the liquid crystal completely even in rapid cooling process and cannot solidify as it is.

We found that the following main-chain smectic liquid crystalline BB-3(1-Me) polyester forms both the smectic CA liquid crystal (LC) glass and the isotropic liquid glass. On gradual cooling from the isotropic liquid phase, the smectic CA phase is formed and solidified without crystallization. On the other hand, rapid cooling from the isotropic state gave a transparent and optically isotropic solid. The glass transition behavior and the enthalpy relaxation of these two glassy solids were investigated with the differential scanning calorimetry (DSC) method.



## Experimental Section

The BB-3(1-Me) polyester was synthesized by melt transesterification of dimethyl 4,4'-biphenylate and 1,3-butanediol with using isopropyl titanate as catalyst. The inherent viscosity of the polymer,  $\eta_{\text{inh}}$ , of  $0.43\text{ dL g}^{-1}$  was measured at  $30\text{ }^{\circ}\text{C}$  by using  $0.5\text{ g dL}^{-1}$  solution in a 60/40 w/w mixture of phenol and tetrachloroethane. The number-average molecular weight,  $M_n = 13\text{ }000$ , and the polydispersity of the molecular weight,  $M_w/M_n = 1.9$ , were determined by gel permeation chromatography (a Showa Denko Shodex K-2004 with a Showa Denko RI-72 detector) in chloroform at  $40\text{ }^{\circ}\text{C}$  on the basis of calibration of standard polystyrene.

\* Corresponding author: Tel +81-3-5734-2834; Fax +81-3-5734-2888; e-mail mtokita@polymer.titech.ac.jp.

DSC measurements were carried out with a Perkin-Elmer Pyris-1 DSC equipped with an Intracooler IIP at a scanning rate of  $10\text{ }^{\circ}\text{C min}^{-1}$  under a flow of dry nitrogen. Temperature-modulated DSC (TMDSC) measurements were performed with the Perkin-Elmer Pyris 1 DSC in dynamic DSC mode. The temperature profile was a saw-tooth modulation at a frequency of  $1.7 \times 10^{-2}\text{ Hz}$  (with a periodic time of 60 s). The modulation amplitude of the temperature oscillation was  $0.5\text{ }^{\circ}\text{C}$ , and the heating rate was  $1\text{ }^{\circ}\text{C min}^{-1}$ . A Perkin-Elmer Pyris software analyzed the heat flow and provided a complex heat capacity,  $C_p^* = C_p' - iC_p''$ .<sup>17</sup> Cross-polarized optical microscopy observations were performed with an Olympus BX-50 optical microscopy equipped with a Mettler FP90/82HT hot stage. Wide-angle X-ray diffraction (WAXD) patterns were recorded on a flat imaging plate by using Ni-filtered  $\text{Cu K}\alpha$  radiation generated by a Rigaku RU-200BH. The sample temperature was regulated with a Mettler FP90/82HT hot stage.

## Results and Discussion

**Characterization for Two Glassy States of BB-3(1-Me) Polyester. a. Smectic LC Glass.** The most principal character of the BB-3(1-Me) polyester is that it forms two distinct solids depending on rate of cooling from the isotropic liquid state. One of the solids was obtained by cooling the isotropic liquid to ambient temperature at rates smaller than  $1\text{ }^{\circ}\text{C min}^{-1}$ . The resulting solid was opaque and optically anisotropic and showed an X-ray pattern characteristic of the smectic LC which included an inner sharp reflection and an outer broad reflection attributed to the smectic layer structure and the liquidlike packing of the mesogens within the layer, respectively (Figure 1a). These show that the solid is the glassy smectic LC. The type of the smectic LC was well identified from the X-ray pattern of the uniaxially oriented fiber which was prepared by stretching the smectic melt. Figure 2 shows the X-ray pattern taken at room temperature with setting the fiber axis in the vertical direction. As previously reported,<sup>11,12,23</sup> stretching of the smectic melt oriented the smectic layer parallel to the elongation flow. The X-ray pattern includes a sharp inner reflection on the equator with a spacing of  $14.0\text{ }\text{\AA}$  while a broad outer reflection with an averaged spacing of  $4.5\text{ }\text{\AA}$  shows intensity maxima in both sides of the meridian, clarifying formation of the smectic CA structure where the mesogens are tilted respect to the layer normal and their tilt direction is alternate between the neighbor layers.<sup>18–24</sup>

**b. Isotropic Liquid Glass.** Another type of solid was obtained when the isotropic melt was rapidly cooled at rates larger than  $50\text{ }^{\circ}\text{C min}^{-1}$ . The solid sample was totally transparent and optically isotropic. Its X-ray diffraction pattern included only an amorphous halo (Figure 1b). The solid was the glassy isotropic liquid. It is noteworthy that in the present BB-3(1-Me) polyester crystallization does not take place at all even if any cooling process applied.

Figure 3 shows the DSC thermograms of the two distinct solids measured on heating at a rate of  $10\text{ }^{\circ}\text{C min}^{-1}$ . As found in Figure 3a, the smectic LC glass showed a simple thermogram including a jump of the heat capacity at around  $81\text{ }^{\circ}\text{C}$  associated with the glass transition and an exothermic peak at  $159\text{ }^{\circ}\text{C}$  due to the isotropization of the liquid crystal. On the other hand, the isotropic liquid glass showed a somewhat complex thermogram. The DSC thermogram shown in Figure 3b includes a step at  $93\text{ }^{\circ}\text{C}$  associated with the glass transition of the isotropic liquid, a sharp exothermic peak at  $110\text{ }^{\circ}\text{C}$ , and finally an endothermic peak at  $159\text{ }^{\circ}\text{C}$ . The exothermic peak following the glass transition

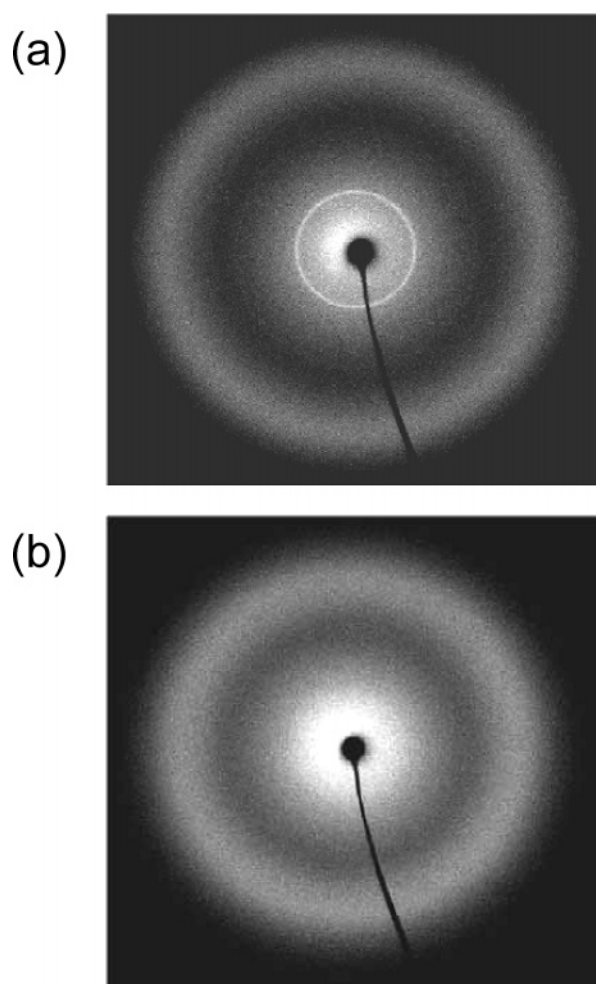


**Figure 1.** X-ray diffraction pattern for the BB-3(1-Me) polyester cooled from the isotropic liquid state to ambient temperature at a rate of  $1\text{ }^{\circ}\text{C min}^{-1}$  (a) and  $100\text{ }^{\circ}\text{C min}^{-1}$  (b).

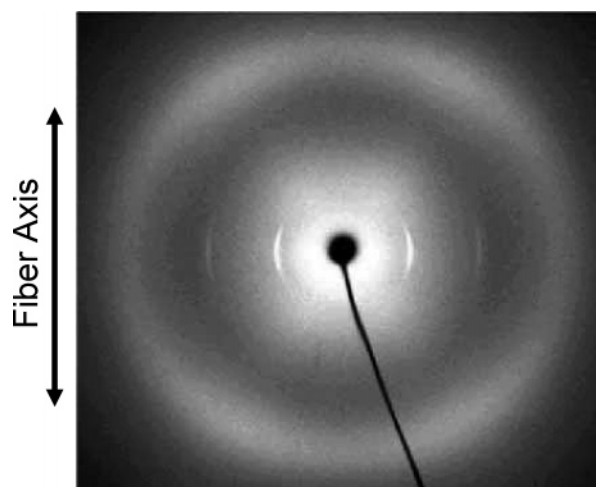


**Figure 2.** X-ray diffraction pattern for the fibrous specimen of the BB-3(1-Me). The sample was prepared by drawing the smectic melt at a rate of ca.  $1\text{ cm min}^{-1}$ . The fiber axis is in the vertical direction.

is assigned to the liquid crystallization of the relaxed isotropic liquid glass, since at this peak temperature of  $110\text{ }^{\circ}\text{C}$ , the sample became opaque and showed birefringence in polarized optical microscopy observation and the X-ray pattern characteristic of the smectic CA structure. The final endothermic peak at  $159\text{ }^{\circ}\text{C}$  is attributed to the isotropization of the smectic LC. The

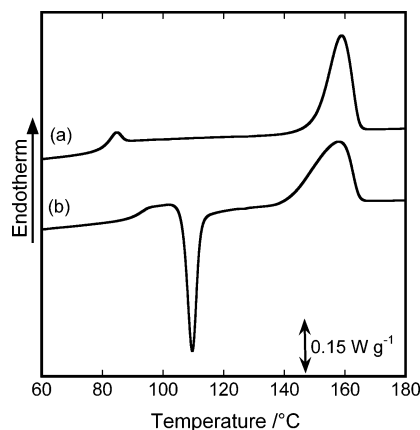


**Figure 3.** DSC heating thermograms of the BB-3(1-Me) polyester measured for the samples cooled from the isotropic liquid state to ambient temperature at rates of (a) 1 °C min<sup>-1</sup> and (b) 100 °C min<sup>-1</sup>. The heating rate was 10 °C min<sup>-1</sup>.

difference in the glass transition temperature ( $T_g$ ) is significant between the two types of glasses:  $T_g$  for the isotropic liquid glass ( $T_g^{\text{iso}}$ ) is 12 °C higher than  $T_g$  for the smectic LC glass ( $T_g^{\text{LC}}$ ). This trend coincides with the conclusion reached in our previous work where the glass transition temperatures were compared between the smectic LC glass and isotropic liquid glass of the homologous series of BB- $n$  polyesters and in the copolyester of BB-6 and poly(hexamethylene 2,6-naphthalene dicarboxylate) with various components.<sup>11</sup> A similar result has been reported for main-chain liquid crystalline polymers which can form these two glassy states.<sup>5,6,14,15</sup>

To investigate their more accurate thermodynamic properties, the specific heat was measured by the TMDSC method. Temperature dependences of  $C_p'$  and  $C_p''$  determined at a frequency of  $1.7 \times 10^{-2}$  Hz are shown in parts a and b of Figure 4, respectively.  $C_p'$  of the two glasses are comparable to each other, showing that similar molecular motions take place in the glassy states. In the glass transition,  $C_p'$  and  $C_p''$  show a jump and a peak, respectively. The TMDSC data clearly show that  $T_g^{\text{iso}}$  (92 °C) is higher than  $T_g^{\text{LC}}$  (81 °C), as found in the conventional DSC thermograms (see Figure 3). The corresponding increase in  $C_p'$  determines  $\Delta C_p$  in the glass transition more accurately than the conventional DSC thermogram because the TMDSC is not influenced by enthalpy relaxation endotherm overlapping with glass transition.<sup>17,25</sup>  $\Delta C_p$  thus estimated were 78.5 and 50.1 J mol<sup>-1</sup> K<sup>-1</sup> for the isotropic liquid glass and the smectic LC glass, respectively. The difference in  $\Delta C_p$  reflects the difference in molecular motion between the isotropic liquid and the smectic LC. In the  $C_p'$  curve of the isotropic liquid glass, the jump is followed by a drop, and the value becomes equal to that of the smectic LC. This drop is thus attributed to the liquid crystallization of the relaxed isotropic liquid glass, but the corresponding exothermic peak observed in the conventional DSC thermogram (Figure 3b) is not found in the  $C_p'$  curve in Figure 4a. It is reasonable since the TMDSC is not influenced by thermal events arising from kinetic process such as the liquid crystallization.<sup>17,25</sup>

The TMDSC thermograms give temperature dependence of the heat capacities of the smectic LC and the isotropic liquid as well as the two glassy states. The

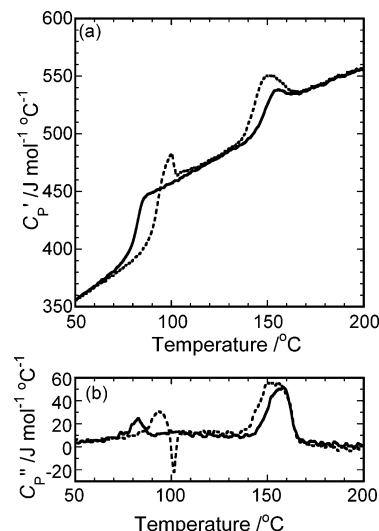


**Figure 4.** Temperature dependence of storage heat capacity  $C_p'$  (a) and loss heat capacity  $C_p''$  (b) determined by temperature-modulated DSC for the BB-3(1-Me) polyester cooled from the isotropic liquid state to ambient temperature at a rate of 1 °C min<sup>-1</sup> (solid curve) and 100 °C min<sup>-1</sup> (dotted curve). The temperature modulation amplitude, the averaged heating rate, and the periodic time were 0.5 °C, 1 °C min<sup>-1</sup>, and 60 s, respectively.

**Table 1. Characterization of the BB-3(1-Me) Polyester**

	$T_g^a$ (°C)	$\Delta C_p^b$ (J mol <sup>-1</sup> K <sup>-1</sup> )	$T_i^a$ (°C)	$\Delta H_i$ (kJ mol <sup>-1</sup> )
smectic LC glass	81	50.1	159	4.47
isotropic liquid glass	93	78.5	159	4.47

<sup>a</sup> Determined by the conventional DSC thermogram measured at 10 °C min<sup>-1</sup>. <sup>b</sup> Determined by the TMDSC thermogram.

**Table 2. Parameters in Eq 2 Describing Temperature Dependence of Enthalpy**

	$a$ (J mol <sup>-1</sup> K <sup>-1</sup> )	$b$ (J mol <sup>-1</sup> K <sup>-2</sup> )	$c$ (J mol <sup>-1</sup> )
isotropic liquid	243	0.665	0.00
smectic LC	1.14	0.921	$2.75 \times 10^4$
isotropic liquid glass	-16.2	1.15	$6.24 \times 10^4$
smectic LC glass	-32.2	1.20	$6.16 \times 10^4$

temperature dependence of  $C_p$  in the measurement temperature range is expressed as

$$C_p = a + bT \quad (1)$$

where  $a$  and  $b$  are the constants determined with temperature dependence of  $C_p'$  and shown in the second and third columns in Table 2. The enthalpy in each state was obtained by integration of eq 1 to estimate the enthalpy-temperature relationship.

$$H = \int C_p dT = aT + bT^2/2 + c \quad (2)$$

Here,  $c$  is the arbitrary constant determined by taking account of continuity in the enthalpy at the glass transition and the enthalpy difference at the isotropic liquid-smectic LC transition and by setting the reference point as the enthalpy of the liquid = 0 J mol<sup>-1</sup> at 0 K. The values of  $c$  determined for the isotropic liquid, the smectic liquid crystal, and their two glasses are presented in the fourth column in Table 2. Figure 5 shows the temperature dependence of the enthalpy estimated for each state by eq 2. Quantitative accuracy of the enthalpy-temperature relationship can be con-



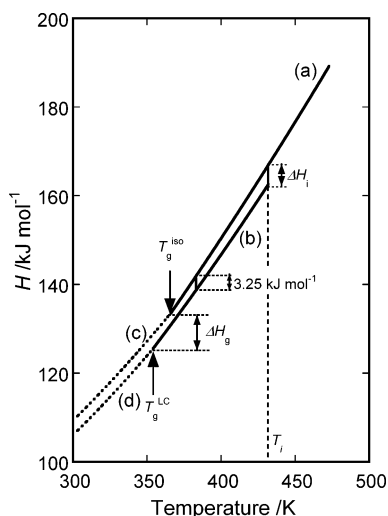


**Figure 5.** Enthalpy–temperature relationship of the BB-3(1-Me) in the isotropic liquid state (a), the smectic LC state (b), the isotropic liquid glass state (c), and the smectic LC glass state (d). The enthalpy was calculated by integration of the heat capacity evaluated by TMDSC (see eq 2). The transition temperatures,  $T_i$ ,  $T_g^{\text{iso}}$ , and  $T_g^{\text{LC}}$  and the isotropization enthalpy,  $\Delta H_i$ , are based on the conventional DSC thermograms in Figure 3. Difference in the enthalpy at 383 K between the isotropic liquid and the smectic LC ( $3.25 \text{ kJ mol}^{-1}$ ) is indicated in the figure for a comparison to the observed enthalpy change in the liquid crystallization taking place at  $110^\circ\text{C}$  ( $383 \text{ K}$ ) on heating the isotropic liquid glass ( $3.11 \text{ kJ mol}^{-1}$ , see Figure 3b).

firmed by comparison of the difference in the enthalpy between the isotropic liquid and the smectic LC at  $110^\circ\text{C}$  ( $3.25 \text{ kJ mol}^{-1}$ , see Figure 5) with the enthalpy change in the liquid crystallization taking place at  $110^\circ\text{C}$  on heating the isotropic liquid glass ( $3.11 \text{ kJ mol}^{-1}$ , see Figure 3b). In the enthalpy–temperature diagram, it is found that the enthalpy at  $T_g$  for the smectic LC is smaller than that for the isotropic liquid and that the difference between them ( $\Delta H_g = 8.02 \text{ kJ mol}^{-1}$ ) is about 2 times larger than the enthalpy change at the isotropic–smectic LC transition ( $\Delta H_i = 4.47 \text{ kJ mol}^{-1}$ ). On the assumption that the enthalpy is proportional to the specific volume, this quantitative result is related to a supposition submitted by Zachmann et al.<sup>5</sup> to explain the lower  $T_g$  of the LC glass: the critical volume at  $T_g$  for the LC is smaller than that for the isotropic liquid, and the difference between them is larger than the volume change at the isotropic–LC transition.

**Two Glass Transitions in Isotropic Liquid.** The two glasses underwent enthalpy relaxation, which was apparent as the endotherm peak appearing immediately after the glass transition in the heating DSC thermogram as seen in Figure 6a. Extent of this relaxation process can be detected by growing of the endothermic peak measured for the glassy solid stored at certain temperature,  $T_a$ , below  $T_g$  for prolonged aging period. The endothermic values were determined by subtracting the DSC curve for the unaged glassy sample from that for the aged sample and are plotted against the aging period in Figure 7. The aging time dependence of the endothermic value is well fitted to the Cowie–Ferguson equation<sup>26</sup>

$$\Delta H(t) = \Delta H_\infty (1 - e^{-(t/\tau)^\beta}) \quad (3)$$

for both these glasses as seen in Figure 7. Thus, we can determine kinetic parameters of average relaxation

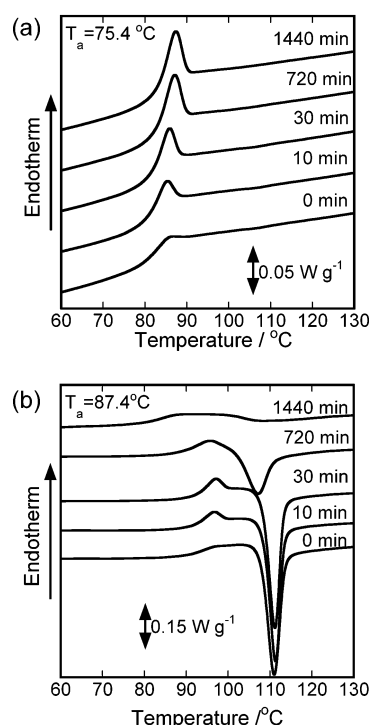


**Figure 6.** DSC thermograms measured by heating the smectic LC glass (a) and the isotropic liquid glass (b) stored at  $75.4$  and  $87.4^\circ\text{C}$ , respectively, for the period indicated in the figure. The heating rate was  $10^\circ\text{C min}^{-1}$ .

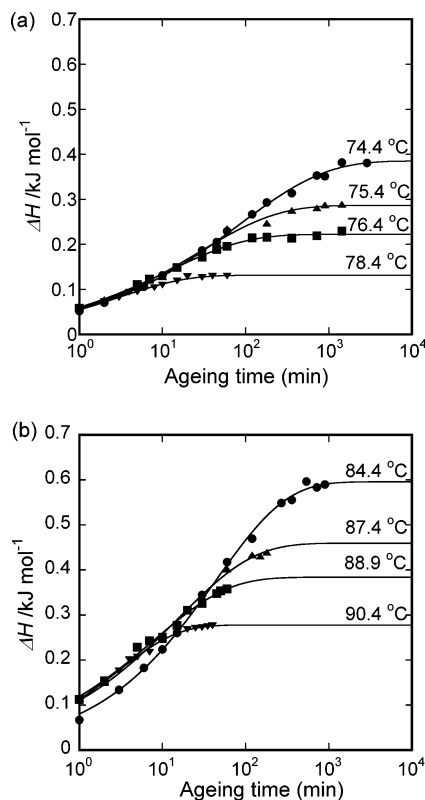


**Figure 7.** Aging time dependence of the enthalpy relaxation endotherm for the smectic LC glass (a) and the isotropic liquid glass (b) at the temperature indicated in the figure. The solid curve shows the validity of Cowie–Ferguson equation.

time,  $\tau$ , and measure of width of the underlying relaxation spectrum,  $\beta$ . Here  $\Delta H_\infty$  is comparable to the value estimated by a simple relationship of  $\Delta H_\infty = \Delta C_p(T_g - T)$ . These parameters are summarized in Table 3. The

**Table 3. Parameters,  $\Delta H_\infty$ ,  $\tau$ , and  $\beta$ , Determined by Fitting of the Aging Time Dependence of the Enthalpy Relaxation Endotherm by Means of the Cowie–Ferguson Relation (3)**

	$T_a$ (°C)	$\Delta H_{\infty, \text{obs}}$ (kJ mol <sup>-1</sup> )	$\Delta H_{\infty, \text{calc}}^a$ (kJ mol <sup>-1</sup> )	$\tau$ (s)	$\beta$
isotropic liquid glass	90.4	0.278	0.204	180	0.609
	88.9	0.384	0.322	460	0.485
	87.4	0.459	0.440	910	0.476
	86.4	0.517	0.518	1330	0.516
	85.4	0.534	0.596	1740	0.523
	84.4	0.596	0.675	2630	0.512
smectic LC glass	78.4	0.132	0.130	190	0.548
	77.4	0.183	0.180	310	0.483
	76.4	0.222	0.230	700	0.466
	75.4	0.287	0.281	1610	0.456
	74.4	0.386	0.331	5030	0.420

<sup>a</sup> The value is calculated using  $\Delta H_\infty = \Delta C_p(T_g - T_a)$ .

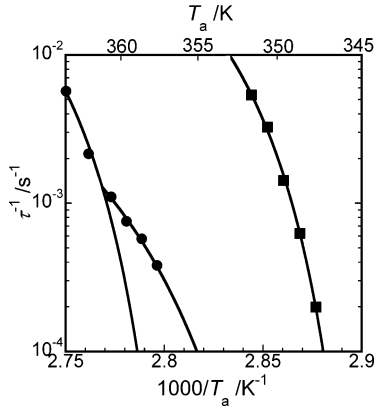


**Figure 8.** Arrhenius plot of the enthalpy relaxation times in the isotropic liquid (circle) and the smectic LC (square). The solid curve shows the validity of VFT description.

relaxation rates depend on extent of undercooling from the glass transition temperature, while  $\beta$  is not significantly dependent on the aging temperature or the type of glassy state.

In Figure 8 the reciprocal of  $\tau$  ( $\tau^{-1}$ ) is plotted against the reciprocal of the aging temperature in units of K. The temperature dependence of  $\tau$  is usually portrayed by the Vogel–Fulcher–Tamman (VFT) relationship:

$$\tau = A \exp\left(\frac{Q}{T - T_0}\right) \quad (4)$$

where  $A$  and  $T_0$  are prefactor and ideal glass temperature, respectively. VFT equation expects a non-Arrhenius relationship between  $\tau^{-1}$  and  $1/T_a$ , where  $\tau^{-1}$  decreases more rapidly with increment in  $T_a^{-1}$  to give a single glass temperature,  $T_0$ . Such a relationship is found for the smectic LC to give  $T_0^{\text{LC}}$  of 343 K (see Figure 8), while for the isotropic liquid, decrease in  $\tau^{-1}$  takes place in two steps; the decrease of  $\tau^{-1}$  in  $T_a^{-1}$  larger than  $2.775 \times 10^{-3} \text{ K}^{-1}$  is less than that in smaller  $T_a^{-1}$ . The data at  $T_a^{-1}$  larger and smaller than  $2.775 \times 10^{-3} \text{ K}^{-1}$  give  $T_{0\text{L}}^{\text{iso}}$  of 343 K and  $T_{0\text{H}}^{\text{iso}}$  of 353 K, respectively.  $T_{0\text{L}}^{\text{iso}}$  is 10 K lower than  $T_{0\text{H}}^{\text{iso}}$  and equal to  $T_0^{\text{LC}}$ . In addition to the enthalpy relaxation, as found in Figure 6b, the aging of the isotropic liquid glass also decreased the exothermic value at 110 °C, showing that the liquid crystallization took place simultaneously in the relaxed isotropic liquid glass. In Figure 9, the enthalpy values of the liquid crystallization are plotted against the aging time and compared with the enthalpy values of the enthalpy relaxation. One can know clearly

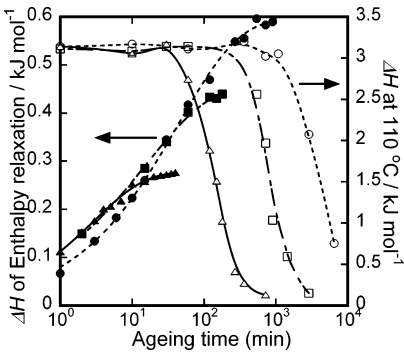


**Figure 9.** Aging time dependences of the enthalpy of the exothermic peak at 110 °C attributed to the liquid crystallization (open symbols). The data shown by circle, square, and triangle are collected at aging temperatures of 84.4, 87.4, and 90.4 °C, respectively. Aging time dependences of the enthalpy relaxation endotherm of the isotropic liquid glass (closed symbols), which are the same as those shown in Figure 7, are also given for a comparison.

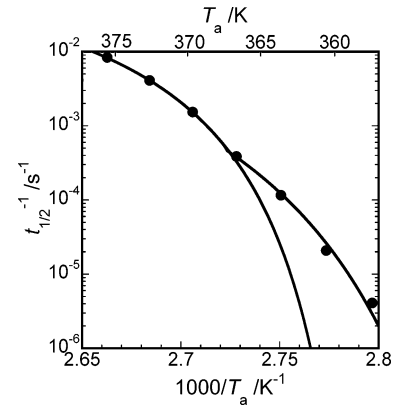


**Figure 10.** Arrhenius plot of the liquid crystallization rate. The solid curve shows the validity of VFT description.

**Table 4. Parameters,  $A$ ,  $Q$ , and  $T_0$ , Determined by Fitting of the Enthalpy Relaxation Rate and the Liquid Crystallization Rate by Means of VFT Relation (4)**

	$A$ (s)	$Q$ (K)	$T_0$ (K)
enthalpy relaxation			
isotropic liquid, $T_a > 360 \text{ K}$	1.15	53.5	353
isotropic liquid, $T_a < 360 \text{ K}$	4.37	96.9	343
smectic LC	1.14	51.3	342
liquid crystallization			
$T_a > 365 \text{ K}$	2.25	80.4	355
$T_a < 365 \text{ K}$	1.46	172	344

that the isotropic liquid glass transformed to the smectic LC after completion of the enthalpy relaxation.

The liquid crystallization process was followed with the fraction conversion ( $X_t$ ), which was estimated from decrease in the area of the exothermic peak due to the liquid crystallization of the unconverted isotropic liquid in the DSC thermograms. We take the inverse of the time at which  $X_t$  is 50% to represent the measure of the transition rate,  $t_{1/2}^{-1}$ . The transition rate shows the VFT-type temperature dependence as shown in Figure 10, giving two glass temperatures of 344 and 355 K. These temperatures are approximate to  $T_{0\text{H}}^{\text{iso}}$  and  $T_{0\text{L}}^{\text{iso}}$  which have been estimated though the enthalpy relaxation rate of the isotropic liquid glass. The appearance of two glass transitions in the isotropic liquid and the coincidence between  $T_{0\text{L}}^{\text{iso}}$  and  $T_0^{\text{LC}}$  thus seem more than casual ones.

Two ideal glass temperatures of isotropic liquid of LC material have been discussed in recent works on glass transition. A mode coupling theory (MCT) developed for spheres has been extended to hard ellipsoids.<sup>27</sup> According to this theory, the ellipsoids with aspect ratio greater than 2.5 (calamitic mesogens) freeze their orientational degree of freedom; the remaining translational degree of freedom still attaches a liquidlike nature to some extent to the system. Temperature scaling analysis for optical heterodyne detected optical Kerr effect data for low molecular weight nematic LC materials have represented two glass transitions of the isotropic liquid.<sup>28</sup> So, the two ideal glass temperatures found in this study may be understood by the same way:  $T_{\text{OH}}^{\text{iso}}$  is attributed to the freezing of molecular orientation fluctuation while  $T_{\text{OL}}^{\text{iso}}$  to the freezing of molecular translation motions. On the other hand, the glass transition in the smectic LC is attributable to the freezing of translational molecular motion within the layer.<sup>11,12</sup> This seems to be a reason why  $T_0^{\text{LC}}$  corresponds to  $T_{\text{OL}}^{\text{iso}}$ .

## Conclusions

We can prepare the isotropic liquid glass and the smectic CA LC glass of the BB-3(1-Me) polyester by changing the rate of cooling from the isotropic melt. The smectic LC glass was prepared by gradual cooling at rates smaller than  $1\text{ }^{\circ}\text{C min}^{-1}$ , while the isotropic liquid glass was obtained by rapid cooling at rates larger than  $50\text{ }^{\circ}\text{C min}^{-1}$ . These two glassy states exhibited different  $T_g$  and  $\Delta C_p$  in the glass transition as determined with the DSC thermograms.  $T_g$  of the isotropic liquid glass of  $93\text{ }^{\circ}\text{C}$  is  $12\text{ }^{\circ}\text{C}$  higher than that of the smectic LC glass of  $81\text{ }^{\circ}\text{C}$ . The corresponding  $\Delta C_p$  of the isotropic liquid glass ( $78.5\text{ J mol}^{-1}\text{ K}^{-1}$ ) is larger than that of the smectic LC glass ( $50.1\text{ J mol}^{-1}\text{ K}^{-1}$ ).

The heat capacity determined by the TMDSC was integrated to depict the enthalpy–temperature diagram of the BB-3(1-Me) in all the states. In the diagram, the enthalpy at  $T_g$  for the smectic LC is smaller than that for the isotropic liquid, and the difference between them is about 2 times larger than the phase transition enthalpy. It is similar to the volume–temperature relationship supposed by Zachmann to explain the lower  $T_g$  of the LC glass.

From the VFT description on temperature dependence of the enthalpy relaxation time for the two glasses, we found a single glass temperature,  $T_0^{\text{LC}}$ , for the smectic LC glass, but two glass temperatures,  $T_{\text{OH}}^{\text{iso}}$  and  $T_{\text{OL}}^{\text{iso}}$ , for the isotropic liquid glass. The existence of the two glass temperatures can be interpreted as a signature of two glass transitions in the isotropic liquid. In the context of a MCT of the glass transition of hard ellipsoid molecule liquid, the lower transition temperature,  $T_{\text{OL}}^{\text{iso}}$ , is connected with the freezing of translational molecular

motions, while the higher one,  $T_{\text{OH}}^{\text{iso}}$ , with the freezing of orientational fluctuation.  $T_{\text{OL}}^{\text{iso}}$  corresponds to  $T_0^{\text{LC}}$ , which seems reasonable since the freezing of translational motion in the layer direction dominantly takes place in the glass transition of the smectic LC.

## References and Notes

- (1) Tsuji, K.; Sorai, M.; Seki, S. *Bull. Chem. Soc. Jpn.* **1971**, *44*, 1452.
- (2) Johari, G. P.; Goodby, J. W. *J. Chem. Phys.* **1982**, *77*, 5165–5172.
- (3) Frosioni, V.; De Petris, S.; Chiellini, E.; Galli, G.; Lenz, R. W. *Mol. Cryst. Liq. Cryst.* **1983**, *98*, 223–242.
- (4) Wunderlich, B.; Grebowicz, J. *Adv. Polym. Sci.* **1984**, *60/61*, 1–59.
- (5) Chen, D.; Zachmann, H. G. *Polymer* **1991**, *32*, 1612–1621.
- (6) Ahumada, O.; Ezquerra, T. A.; Nogales, A.; Baltà-Colleja, F. J.; Zachmann, H. G. *Macromolecules* **1996**, *29*, 5002–5009.
- (7) Welder, W.; Demus, D.; Zashcke, H.; Mohr, K.; Schäfer, W.; Weissflog, W. *J. Mater. Chem.* **1991**, *1*, 347–356.
- (8) Welder, W.; Hartmann, P.; Bakowsky, U.; Diele, S.; Demus, D. *J. Mater. Chem.* **1992**, *2*, 1195–1204.
- (9) Gonzalez, Y.; Palacios, B.; Pérez Jubindo, M. A.; Rosario de la Fuente, M.; José Luis Serrano, *Phys. Rev. E* **1995**, *52*, R5764–R5767.
- (10) Palacios, B.; De La Fuente, M. R.; Pérez Jubindo, M. A.; Ros, M. B. *Liq. Cryst.* **1997**, *23*, 349–355.
- (11) Tokita, M.; Osada, K.; Watanabe, J. *Polym. J.* **1998**, *30*, 589–595.
- (12) Osada, K.; Koike, M.; Tagawa, H.; Tokita, M.; Watanabe, J. *Macromol. Chem. Phys.* **2004**, *205*, 1051–1057.
- (13) del Campo, A.; Ezquerra, T. A.; Wilbert, G.; Passmann, M.; Zentel, R. *Macromol. Chem. Phys.* **2002**, *203*, 2089–2094.
- (14) del Campo, A.; Bello, A.; Pérez, E.; García-Bernabé, A.; Díaz Calleja, R. *Macromol. Chem. Phys.* **2002**, *203*, 2508–2515.
- (15) García-Bernabé, A.; Díaz Calleja, R.; Sanchis, M. J.; del Campo, A.; Bello, A.; Pérez, E. *Polymer* **2004**, *45*, 1533–1543.
- (16) Chen, S. H.; Phillip Chen, H. M.; Geng, Y.; Jacob, S. D.; Marchell, K. L.; Blanton, T. N. *Adv. Mater.* **2003**, *15*, 1061–1065.
- (17) Schawe, J. E. K. *Thermochim. Acta* **1995**, *260*, 1–16.
- (18) Watanabe, J.; Hayashi, M. *Macromolecules* **1988**, *21*, 278–280.
- (19) Watanabe, J.; Hayashi, M. *Macromolecules* **1989**, *22*, 4083–4088.
- (20) Watanabe, J.; Kinoshita, S. *J. Phys. (Paris)* **1992**, *2*, 1237–1245.
- (21) Watanabe, J.; Hayashi, M.; Nakata, Y.; Niori, T.; Tokita, M. *Prog. Polym. Sci.* **1997**, *22*, 1053–1087.
- (22) Tokita, M.; Osada, K.; Watanabe, J. *Liq. Cryst.* **1998**, *24*, 477–480.
- (23) Tokita, M.; Osada, K.; Watanabe, J. *Polym. J.* **1998**, *30*, 687–690.
- (24) Tokita, M.; Tokunaga, K.; Funaoka, S.; Osada, K.; Watanabe, J. *Macromolecules* **2004**, 2527–2531.
- (25) Reading, M. *Trends Polym. Sci.* **1993**, *1*, 248–253.
- (26) Brunacci, A.; Cowie, J. M. G.; Ferguson, R.; McEwen, I. J. *Polymer* **1997**, *38*, 865–870.
- (27) Letz, M.; Schilling, R.; Latz, A. *Phys. Rev. E* **2000**, *62*, 5173–5178.
- (28) Cang, H.; Li, J.; Novikov, V. N.; Fayer, M. D. *J. Chem. Phys.* **2003**, *119*, 10421–10427.

MA048769+